THE JOURNAL OF BIOLOGICAL CHEMISTRY
Vol. 278, No. 41, Issue of October 10, pp. 40169–40176, 2003

Printed in U.S.A.

Cofilin Interacts with ClC-5 and Regulates Albumin Uptake in Proximal Tubule Cell Lines*

Received for publication, July 21, 2003, and in revised form, August 5, 2003
Published, JBC Papers in Press, August 6, 2003, DOI 10.1074/jbc.M307890200

Deanne H. Hryciw‡§, Yinghong Wang‡, Olivier Devuyst¶, Carol A. Pollock‖, Philip Poronnik§‖, and William B. Guggino‡

From the ‡Department of Physiology, School of Medicine, Johns Hopkins University, Baltimore, Maryland 21205, ¶Division of Nephrology, Université Catholique de Louvain Medical School, B-1200 Brussels, Belgium, ‖Department of Medicine, University of Sydney, Royal North Shore Hospital, St Leonards 2065, Australia, and §School of Biomedical Sciences, University of Queensland, St Lucia 4072, Australia

Receptor-mediated endocytosis is a constitutive high capacity pathway for the reabsorption of proteins from the glomerular filtrate by the renal proximal tubule. ClC-5 is a voltage-gated chloride channel found in the proximal tubule where it has been shown to be essential for protein uptake, based on evidence from patients with Dent's disease and studies in ClC-5 knockout mice. To further delineate the role of ClC-5 in albumin uptake, we performed a yeast two-hybrid screen with the C-terminal tail of ClC-5 to identify any interactions of the channel with proteins involved in endocytosis. We found that the C-terminal tail of ClC-5 bound the actin depolymerizing protein, cofilin, a result that was confirmed by GST-fusion pulldown assays. In cultured proximal tubule cells, cofilin was distributed in nuclear, cytoplasmic, and microsomal fractions and co-localized with ClC-5. Phosphorylation of cofilin by overexpressing LIM kinase 1 resulted in a stabilization of the actin cytoskeleton. Phosphorylation of cofilin in two proximal tubule cell models (porcine renal proximal tubule and opossum kidney) was also accompanied by a pronounced inhibition of albumin uptake. This study identifies a novel interaction between the C-terminal tail of ClC-5 and cofilin, an actin-associated protein that is crucial in the regulation of albumin uptake by the proximal tubule.

One of the major roles of the cortical nephron is to reabsorb proteins such as albumin from the glomerular filtrate. It is estimated that the kidneys reabsorb up to several grams of albumin/day, a process that is achieved in the proximal tubule by highly active and tightly regulated receptor-mediated endocytosis involving the megalin-cubulin scavenger receptor complex (1). It is now clear that the uptake of albumin requires the coordinated activity of a number of proteins that may exist in a macromolecular complex within the endosome. This complex seems to include the albumin receptor megalin, V-type H^+-ATPase, Na^+-H^+ exchanger isoform 3 (NHE3),[1] and the Cl^- channel ClC-5 (2–4). These proteins have defined transport functions that account for the various ion movements required during endosomal formation and acidification. V-type H^+-ATPase plays a critical role in the acidification of the endosome, leading to dissociation of the albumin from megalin and its subsequent degradation in the lysosome (4). ClC-5 is thought to be essential to provide the necessary anion shunt to neutralize the positive charge caused by H^+ movement by the V-type H^+-ATPase during the acidification of the endosome as it progresses to the lysosome (5, 6). NHE3 may play a facilitatory role in mediating the initial acidification process by exchanging the high Na^+ for H^+ in the newly formed endosome as it buds away from the membrane (3).

The functional importance of these proteins in mediating albumin uptake has been shown in genetic disorders and in cell culture models. ClC-5 is essential for albumin uptake. In Dent's disease, which is caused by mutations in ClC-5, one of the key outcomes is low molecular weight proteinuria (6). Furthermore, ClC-5 knockout mice also have proteinuria and in both of these cases, the proteinuria is caused by defective protein uptake in the proximal tubule (6, 7). This effect is thought to be caused by the key role of ClC-5 as an anion shunt, as the rate of acidification of apical vesicles derived from ClC-5 knockout mice is significantly lower than that observed in vesicles derived from wild-type mice (6). As a result, the uptake of markers of receptor-mediated and fluid phase endocytosis is severely impaired in the kidneys of ClC-5 knockout mice (6, 7). In addition, NHE3 activity also seems to be involved in albumin uptake. In cultured opossum kidney (OK) cells or porcine renal proximal tubule (LLC-PK1) cells (8), inhibition of NHE3 with 5-(*N*-ethyl-*N*-isopropyl)-amiloride inhibits albumin uptake, and in OK cells lacking NHE3, albumin uptake is abolished (3). In contrast to ClC-5 knockout mice, however, there are no reports of proteinuria in NHE3 knockout mice, which argues against an obligate role for NHE3 in albumin uptake *in vivo*. In addition to mediating ion transport, both ClC-5 and NHE3 possess large intracellular C-terminal tails which can interact with scaffold or regulatory proteins in the cytoplasm, an essential component of the endocytotic pathway (9). For example, the binding of sodium-hydrogen exchange regulatory factor to the PDZ binding domain of NHE3 (the subject of extensive study) mediates the interaction of NHE3 with the actin cytoskeleton (10, 11) and forms localized signaling complexes for regulation by protein kinase A (12) and PI-3 kinase (13). In addition, NHE3

* This work was funded by National Institutes of Health Grants DK32753 and HL47122 (to W. B. G.), Forton Foundation Grant ARC 00/05-260, Fondation pour la Recherche Scientifique Medicale (to O. D.), the National Health and Medical Research Council of Australia (to C. A. P. and P. P.), and Juvenile Diabetes Foundation International (to P. P. and C. A. P.). The costs of publication of this article were defrayed in part by the payment of page charges. This article must therefore be hereby marked "*advertisement*" in accordance with 18 U.S.C. Section 1734 solely to indicate this fact.

** To whom correspondence should be addressed. Tel.: 410-955-7166; Fax: 410-955-0461; E-mail: wguggino@jhmi.edu.

[1] The abbreviations used are: NHE3, Na^+-H^+ exchanger isoform 3; ClC-5, voltage-gated Cl^- channel; OK, opossum kidney; LLC-PK1, porcine renal proximal tubule; PI, phosphatidylinositol; LIMK-1, LIM kinase 1; GST, glutathione *S*-transferase; PBS, phosphate-buffered saline; TRITC, tetramethylrhodamine isothiocyanate; MOPS, 4-morpholinepropanesulfonic acid.

has been shown to interact with megalin by means of C-terminal interactions (14).

In contrast, despite ClC-5 being essential for the uptake of albumin, little is known about the functional interactions of the intracellular C terminus of ClC-5. The terminus contains a number of potential binding signals for regulatory molecules, including cystathione-β synthase domain (15, 16), a PY motif (17), and a PDZ binding domain. Thus, it is possible that ClC-5 may play a crucial role in regulating endocytosis by means of C-terminal interactions with other proteins involved in the endocytotic pathway in the proximal tubule. We have recently shown that horseradish peroxidase infused into the kidneys of ClC-5 knockout mice remains trapped in a sub-plasmalemmal pre-endocytotic compartment and fails to enter the endosomal pathway proper (7). This finding suggests that the endocytotic defect may also be occurring earlier, at the formation of the nascent endosome, and that this may be because of interactions of ClC-5 with proteins involved in regulating the endocytotic process. Another possibility is trafficking, with evidence for this role for ClC-5 in the trafficking of other membrane proteins provided by studies in patients with Dent's disease, where defective ClC-5 resulted in the mis-trafficking of the V-type H^+-ATPase (18) and in ClC-5 knockout mice, where mis-trafficking results in reduced levels of megalin/cubulin at the plasma membrane (19).

The internalization of the albumin-megalin complex occurs by means of clathrin-coated pits (20). The processes by which clathrin-coated pits are formed, recruit cargo, and detach as nascent endosomes are well characterized. The series of events, however, that allows the nascent endosome to pass through the cortical actin web into the cytoplasm are less well understood. Although albumin endocytosis is known to require intact cytoskeletal structures (21), the exact nature of the role of the cytoskeleton remains to be elucidated. The cytoskeleton itself may present a physical barrier to the endocytotic machinery (22, 23), and therefore some localized remodeling of the network filaments must occur for the endosome to pass into the cytoplasm. In fact, it has been observed that the area in the immediate vicinity of clathrin-coated pits is largely devoid of actin filaments (24). One way this can be achieved is by the dissolution of actin filaments in the immediate vicinity of the endosome by actin depolymerizing proteins. The rapid turnover of actin filaments and the tertiary meshwork formation is regulated by a variety of actin-binding proteins such as the actin-depolymerizing factor/cofilin proteins (25). These proteins are potent regulators of actin filament dynamics in eukaryotic cells and mediate the severing and depolymerization of actin. The actin-depolymerizing factor/cofilin family has been shown to play a crucial role in mediating microvillar breakdown and rapid cytoskeletal alterations in ischemic and ATP-depleted proximal tubule cells (26).

Therefore, we performed yeast two-hybrid screens to determine whether the C terminus of ClC-5 interacts with proteins involved in endocytosis. This revealed a novel interaction between the C terminus of ClC-5 and the actin binding protein, cofilin. These proteins co-localize in vesicles containing the endosomal marker AP-2. Furthermore, we demonstrated that phosphorylation of cofilin by LIM kinase inhibits albumin uptake in two model proximal tubule cell lines, namely LLC-PK1 and OK cells. Our data suggest that the interaction between cofilin and ClC-5 plays a critical regulatory role in the reabsorption of low molecular weight proteins in the proximal tubule.

MATERIALS AND METHODS

Cells and Antibodies—The LLC-PK1 and OK cell lines were obtained from American Type Culture Collection. LLC-PK1 cells were maintained in Dulbecco's modified Eagle's medium supplemented with 10% fetal bovine serum, 1% penicillin and streptomycin, whereas OK cells were maintained in Dulbecco's modified Eagle's medium/Ham's-F12 media supplemented with 10% fetal bovine serum, 1% penicillin and streptomycin and incubated at 37 °C in 5% CO_2. Polyclonal antibodies against the N terminus of human ClC-5 were generated in rabbits immunized with keyhole limpet hemocyanin conjugated with synthetic peptide (CKSRDRDRHREITNKS), corresponding to amino acids 26–40 near the N terminus of ClC-5 with an additional N-terminal cysteine. Anti-ClC-5 IgG was affinity-purified with a column containing 5 mg of peptide (Eurogenetec, Seraing, Belgium). Anti-glutathione *S*-transferase (GST) was purchased from Amersham Biosciences. Anti-cofilin was purchased from Cytoskeleton Inc. (Denver, CO). Anti-c-*myc* was purchased from Roche Applied Science. Anti-actin was purchased from Chemicon (Temecula, CA). TRITC-phalloidin was purchased from Sigma. All secondary alkaline phosphatase-conjugated antibodies were obtained from Bio-Rad. Labeled secondary antibodies were obtained from Jackson ImmunoResearch (West Grove, PA).

Cloning of Human ClC-5 cDNA and Construction of Bait Vectors—Human ClC-5 (hClC-5) cDNA was isolated from a human kidney Matchmaker cDNA library (Clontech, Palo Alto, CA) using reverse transcriptase-PCR with the forward and reverse primers and cloned into the pGEM-T Easy Vector (Promega, Madison, WI). Plasmid DNA was screened for the desired insert by restriction analysis, sequenced entirely by automated DNA sequencing (performed at the Johns Hopkins University Biosynthesis and Sequencing Facility), and confirmed to be human ClC-5. The full-length C-terminal tail of ClC-5 (amino acids 563–746) was then cloned into the two-hybrid bait vector pAS2-1 and designated FBD. In addition, the C-terminal tail was divided into three regions and cloned into pAS2-1. These three regions isolated the two CBS regions (CBS1, amino acids 595–645, and CBS2, amino acids 686–733) and the region encompassing the PY domain (amino acids 646–685).

Yeast Two-hybrid Analysis—Two-hybrid analysis was performed by using the Matchmaker human kidney cDNA library (Clontech) and screened for interacting proteins by transformation of Y190 yeast on selective minimal synthetic dropout medium (Leu-, Trp-, His-, 35 mM 3-amino-1,2,4-triazole) at 30 °C for 2–7 days. A β-galactosidase assay confirmed the interactions. To confirm the interactions with cofilin, a bait pACT2 vector expressing cofilin was created (Cofilin).

GST-cofilin Pulldown Assay—Cofilin was cloned into the pGEX-6P-1 (Amersham Biosciences) vector using the *Eco*RI and *Xho*I sites (GST-cofilin). The GST-cofilin fusion protein was produced by using the GST purification kit (Amersham Biosciences) following the manufacturer's instructions. Expression of the GST fusion protein was induced with 1 mM isopropyl-1-thio-β-D-galactopyranoside, cells were lysed by sonication, and the GST fusion protein was purified by using a glutathione-Sepharose 4B column. For the pulldown assay, 50 μg of GST or GST-cofilin fusion protein was incubated with glutathione-Sepharose 4B beads (Amersham Biosciences) for 3 h at 4 °C. The beads were then washed by centrifugation and incubated with ~1 mg of lysate from LLC-PK1 cells at 4 °C for 18 h. The beads were then washed, the samples were eluted into Laemmli gel sample buffer, separated on a 12% SDS-PAGE, and transferred to polyvinylidene difluoride membranes. Western blotting was performed using the anti-ClC-5 and anti-GST antibodies, and the blots were detected by using secondary antibodies conjugated to alkaline phosphatase.

Intracellular Distribution of Cofilin—LLC-PK1 cells were scraped into suspension buffer (10 mM Tris-HCl, 1 mM EDTA), and the membranes were disrupted by passing the sample through a 25-gauge needle 20 times. Nuclear, cytosolic, and microsomal fractions were harvested as described previously (27). Briefly, the nuclei were harvested by centrifugation at 10,000 $\times$ *g*, and the postnuclear supernatant was centrifuged at 100,000 $\times$ *g* for 90 min. The pellet (microsomal fraction) was suspended in suspension buffer. The supernatant was centrifuged at 100,000 $\times$ *g* for 45 min, and the subsequent supernatant was collected (cytosolic fraction). Equal volumes of protein fractions were resolved on 4–15% Tris-HCl gradient gels, and cofilin was detected by Western blotting as described above.

Confocal Microscopy of Endogenous ClC-5 and Cofilin—Cells (LLC-PK1 or OK) grown on glass coverslips were fixed in 4% paraformaldehyde in 0.1 M phosphate-buffered saline (PBS), pH 7.2, for 10 min and permeabilized for 1 min with an ice-cold solution of 0.1% (v/v) Triton X-100 in PBS, 1% (v/v) normal donkey serum. Cells were washed three times in PBS, and the non-antigenic sites were blocked with 1% (v/v) normal donkey serum for 30 min. Incubation with the primary antibodies was performed at 37 °C for 30 min. To co-label the samples for ClC-5 and cofilin, the following protocol was employed (28). Samples were first

incubated with rabbit anti-ClC-5, then with goat anti-rabbit to block any non-bound sites on the rabbit antibody, and finally with donkey anti-goat conjugated to TRITC. Cofilin was then labeled cofilin with the anti-cofilin antibody and subsequently with a Cy2-conjugated goat anti-rabbit secondary. Between each antibody exposure, samples were washed three times for 10 min in PBS to eliminate nonspecific binding of the antibodies and cross-reactivity. Samples were then mounted in Vectashield (Vector, Burlingame, CA) and viewed with a Noran Oz confocal microscope fitted with a 100× oil immersion objective.

Analysis of LIMK-1-transfected Cells—LLC-PK1 cells were transiently transfected with a c-*myc*-tagged LIMK-1 in pCDNA3 (kindly provided by Dr. Pico Caroni, Friedrich Miescher Institute, Switzerland) using NovaFector (Venn Nova, Pompano Beach, FL). Expression of the c-*myc* LIMK-1 was confirmed by using a monoclonal c-*myc* antibody Western blot analysis. An antibody that specifically binds to phosphorylated cofilin (29) (generously provided by Dr. James Bamburg, Colorado State University, Fort Collins, CO) was used to detect the phosphorylated cofilin. Equal loading of samples was confirmed by using an actin antibody as a control. To determine the effects of LIMK-1 overexpression on the actin distribution, transfected cells were fixed, permeabilized, and labeled with TRITC-phalloidin (1 μg/ml) for 20 min, and LIMK-1 was detected by using the c-*myc* antibody as described above.

Albumin Uptake—We used two different methods to measure the effects of LIMK-1 overexpression on albumin uptake in cultured proximal tubule cells. The first method used a modified albumin uptake method in OK cells, a cell line commonly used for the study of proximal tubule albumin uptake (3, 9, 30). Control (mock-transfected) OK cells or cells transfected with c-*myc*-LIMK-1 were grown in 48-well plates for 7 days. In the final 48 h prior to experimentation, cells were changed to serum-free medium. Then cells were exposed to 50 μg/ml albumin conjugated to Texas Red (TR-albumin, Molecular Probes, Eugene, OR) under different conditions for 120 min. As a control to determine the level of endocytosis dependent on the intact cytoskeleton, some cells were pre-treated with latrunculin A (1.5 μM) for 60 min before exposure to TR-albumin. Nonspecific binding was determined in cells exposed to albumin for 1 min, a time at which no albumin uptake could be detected. At the end of the uptake period, cells were washed in HEPES buffer, pH 6, at 4 °C and then lysed in MOPS buffer (20 mM MOPS with 0.1% Triton X-100). The TR-albumin fluorescence was determined by using a Fusion spectrophotometer (Hewlett Packard, Blackburn, Victoria, Australia) at 580 nm excitation and 630 nm emission wavelengths. TR-albumin uptake was standardized to total cellular protein, and the amount of fluorescence/μg of cellular protein was adjusted for background.

To confirm the effects of LIMK-1 overexpression on albumin uptake in proximal tubule cells, we used single cell confocal microscopic analysis and a different proximal tubule cell line, LLC-PK1 (31). LLC-PK1 cells have also been shown to take up albumin at a rate comparable with OK cells. LLC-PK1 cells grown on coverslips and transfected with c-*myc*-LIMK-1 were exposed to fluorescein isothiocyanate-albumin (10 mg/ml) at 37 °C and incubated at times from 0 to 15 min. At the end of each time point, the cells were washed thoroughly in PBS and fixed as described above for confocal microscopy. Expression of c-*myc* LIMK-1 was detected with anti-c-*myc* antibody, and secondary antibody was conjugated to Cy3. The rate of albumin uptake was measured by averaging the fluorescence intensity of 10 individual control cells at each of the time points using Interaction and Presentation Laboratory software version 3.5. Parallel experiments were performed on untransfected control cells, on cells held at 4 °C to abolish endocytosis, and on cells pretreated with 30 μM cytochalasin D for 30 min to disrupt the actin cytoskeleton and inhibit endocytosis. For the LIMK-1 transfected cells, only those cells determined to be positive for c-*myc* LIMK-1 expression were analyzed.

Detection of LIMK-1 and LIMK-2 by Reverse Transcriptase-PCR Analysis—RNA was extracted from OK cells using Trizol reagent and the manufacturer's protocol. 2 μg of RNA was reverse transcribed using Superscript III (Invitrogen) and an aliquot analyzed by PCR using the following primers: LIMK-1 forward, 5′-GTGATGGGGACACCTACACACTGG-3′; LIMK-1 reverse, 5′-GGAGCAGGCGGCTGGTCTCCTGG-3′; LIMK-2 forward, 5′-TCCTCCTCCCCATTTCCGGGCTCC-3′; LIMK-2 reverse, 5′-TCTGTGGAGAGTCTCTCAAACATG-3′. β-Actin was amplified as a control for reverse transcriptase-PCR.

Quantification of Results and Statistical Analysis—Densitometric analysis of the Western blot data was performed using Fujifilm ScienceLab 99 Image Gauge (version 3.3). The percent co-localization between cofilin and ClC-5 was determined by using the Ultraview software co-localization function. The data were obtained from eight images composed of at least five cells in each view and reported as percent co-localization ± S.E. Statistical analyses of the data were performed with two-tailed Student's paired *t* tests; $p < 0.05$ was considered significant.

TABLE I

Yeast two-hybrid analysis of the interaction between ClC-5 and cofilin

Yeast two-hybrid analysis identifies an interaction between ClC-5 and cofilin. Fragments, as well as the entire C terminus of ClC-5, were cloned into pACT2 and pAS2–1 vectors. Yeast two-hybrid analysis was performed using the Matchmaker system. Interactions were deemed positive by growth on selective media and a positive β-galactosidase assay. Both the full-length cofilin as well as a clone that contained an additional 17 amino acids in frame from the 5′-untranslated region (clone 82–5) were able to interact with the C terminus of ClC-5 (FBD). Smaller regions of the C terminus of ClC-5, namely CBS1, CBS2, and PY, were not able to bind to cofilin.

pACT2	pAS2–1	Interaction?
No insert	FBD	No
Clone 82–5	FBD	Yes
Cofilin	FBD	Yes
Cofilin	CBS1	No
Cofilin	CBS2	No
Cofilin	PY	No
Cofilin	No insert	No

RESULTS

Yeast Two-hybrid Screen—The yeast two-hybrid screen of a human kidney cDNA library using the C terminus of human ClC-5 revealed an interaction with a clone (82-5) that coded for non-muscle isoform of cofilin (cofilin1) (GenBank™ accession number NM_005507). This cDNA was subcloned, and a subsequent two-hybrid screen confirmed the interaction between cofilin and ClC-5 (Table I). We then used the C-terminal fragments to attempt to identify the residues responsible for the interaction with cofilin. Unlike the interaction with the full-length tail, we found that none of the C-terminal fragments (CBS1, CBS2, or PY) interacted with cofilin in the two-hybrid assay.

GST Pulldown—To confirm an interaction between cofilin and ClC-5 in mammalian cells, we performed GST pulldowns. A GST-cofilin fusion protein was produced in BL-21 *Escherichia coli* and bound to glutathione-Sepharose beads. Lysate from LLC-PK1 cells was applied to the beads, and after washing, the protein bound to the beads was eluted, separated by SDS-PAGE, and Western blotted. The Western blots were then probed with the antibody against ClC-5. In control lysates incubated with GST alone, there was a nonspecific band at ~50 kDa (data not shown). However, in lysates incubated with GST-cofilin, there was a clear band at ~85 kDa corresponding to ClC-5 (Fig. 1*A*). This experiment was performed three times, and it was found that there was a significant level ($p < 0.001$) of ClC-5 binding to GST-cofilin compared with GST alone (Fig. 1*B*). These data confirm the interaction between endogenous ClC-5 and cofilin in cells of proximal tubule origin.

Cellular Distribution of Cofilin—Cofilin is widely distributed throughout the cytoplasm and nuclei of cells and can translocate to the plasma membrane in response to various stimuli (23). Cofilin has no predicted transmembrane domains; therefore, its association with cellular membranes is caused by interactions with proteins in or associated with these membranes. Therefore, we investigated the distribution of cofilin in nuclear, cytoplasmic, and microsomal fractions of LLC-PK1 cells. We found that in addition to being in the nucleus and cytoplasm, a significant fraction of the cofilin was associated with the microsomal membranes (Fig. 2). This association indicated that cofilin must be associating constitutively with other membrane-bound proteins in these cells, which is consistent with the high levels of ClC-5 found in these fractions.

Subcellular Localization of Cofilin and ClC-5—We then per-

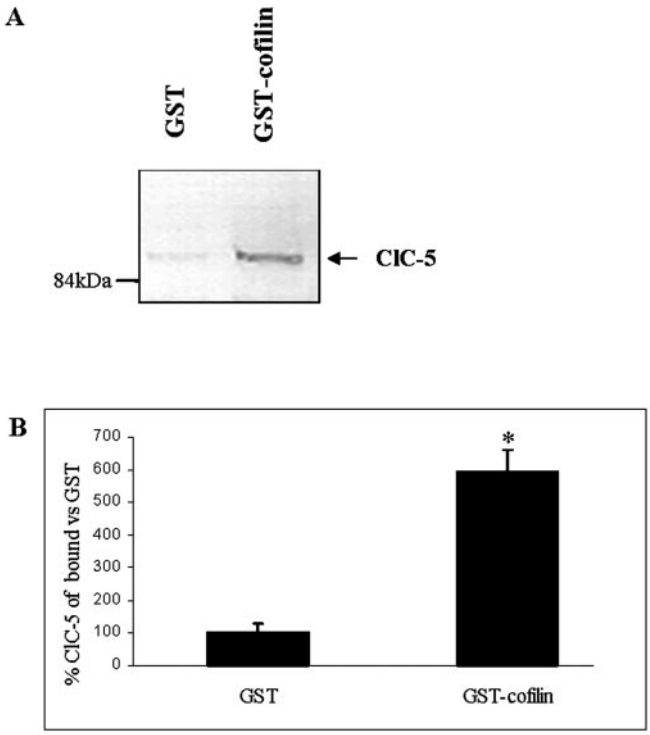

FIG. 1. **ClC-5 C terminus binding to cofilin.** LLC-PK1 cell lysate was incubated with either GST or GST-cofilin-agarose beads. *A*, Western blot showing GST-cofilin binding to ClC-5 in LLC-PK1 lysate. *B*, densitometric analysis showing a significant (*, $p < 0.05$; $n = 3$) increase in the amount of ClC-5 binding to GST-cofilin compared with the GST alone.

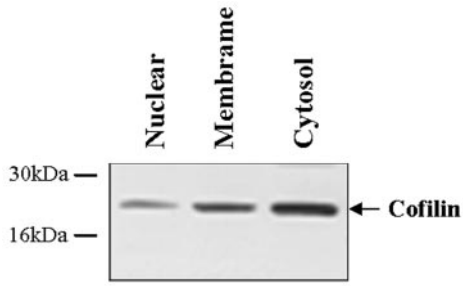

FIG. 2. **Cofilin distribution in the nuclear, cytoplasmic, and microsomal fractions.** LLC-PK1 cells fractionated and run on a Western blot. Cofilin was found in the nuclear, microsomal (*Membrane*), and cytosol fractions.

formed dual wavelength confocal microscopy on permeabilized cells using antibodies against cofilin and ClC-5 to demonstrate co-localization. We found that endogenous ClC-5 occurred in punctate structures throughout the cytoplasm, which is consistent with its presence in recycling endosomes (Fig. 3*A*). Cofilin also showed a similar distribution (Fig. 3*B*), and when the two images were overlaid, there was clear co-localization of the two proteins (Fig. 3*C*). Pixel density analysis confirmed that there was a significant degree of co-localization of 63.0 ± 11.6% ($p < 0.005$; $n = 10$). Furthermore, we also found that the marker of budding endosomes, AP-2 (Fig. 3*D*), also co-localized with cofilin and ClC-5 (Fig. 3*E*). Analysis of a *z*-scan of polarized LLC-PK1 cells indicated that ClC-5 (Fig. 3*F*) and cofilin (Fig. 3*G*) co-localized in the subapical region of the cell (Fig. 3*H*).

Phosphorylation of Cofilin by LIMK-1—We then investigated whether we could modulate the activity of cofilin in cultured proximal tubule cells. Cofilin is a phosphoprotein which, when phosphorylated, is unable to interact with actin microfilaments. Cofilin is presently the only known substrate of LIM kinase, of which there are two isoforms, LIMK-1 and LIMK-2 (31). In OK cells, we detected transcript for LIMK-1 but could not detect any RNA transcript for LIMK-2 (data not shown). LLC-PK1 cells were transfected with c-*myc* epitope-tagged LIMK-1 for 48 h, and Western blots were performed on the cellular lysates. An anti-c-*myc* antibody confirmed that there was a significant expression of LIMK-1 in the cells (Fig. 4*A*). We then probed the same cellular lysates on Western blots by using an antibody directed against the phosphorylated form of cofilin. The over-expression of LIMK-1 in LLC-PK1 cells resulted in a significant increase in the phosphorylation level of endogenous cofilin ($p < 0.05$; $n = 3$) (Fig. 4, *B* and *C*). It is important to note that the transfection efficiency of these experiments was approximately ~30–50% as assessed by transfection with green fluorescent protein (data not shown); therefore, the increase in the phosphorylation of cofilin measured was a considerable underestimate of the increase in transfected cells, as the lysate included both transfected and untransfected cells.

Next we determined whether phosphorylation of cofilin by LIMK-1 resulted in any alterations in the morphology of the actin cytoskeleton. OK cells transfected with c-*myc*-LIMK-1 were fixed and double-labeled with anti-c-*myc* antibody and TRITC-phalloidin. Confocal microscopy was used to determine the changes in the actin cytoskeleton in cells exposed to the actin filament disrupting agent latrunculin A or in cells expressing LIMK-1. In control cells, there was pronounced actin staining at the peripheral corona as well as at the bases of the microvilli (Fig. 5*A*). The *z* axis scans revealed the typical peripheral distribution of actin at the apical and basolateral domains (Fig. 5*B*). In contrast, in cells treated with latrunculin A, the microfilaments were severely disrupted with staining, almost disappearing from the apical domain and the microvillar region (Fig. 5, *C* and *D*). In cells expressing LIMK-1, there was an apparent increase in TRITC-phalloidin staining at the cell periphery of the cells consistent with stabilization of actin filaments (Fig. 5, *E–H*). There was also a pronounced increase in the amount of actin at the base of the microvilli compared with control cells (Fig. 5, *E* and *F*; *cf.* Fig. 5*A*), indicating stabilization of the microfilaments in the regions where albumin uptake is thought to occur.

ClC-5 is essential for albumin uptake, and we demonstrated that ClC-5 binds to cofilin. Therefore, we investigated whether altering the phosphorylation state of cofilin with LIMK-1 and stabilization of actin microfilaments had any effect on albumin endocytosis in cultured proximal tubule cells. In OK cells expressing LIMK-1, there was a significant reduction in the uptake of TR-albumin (Molecular Probes) to 67.0 ± 3.5% ($n = 4$; $p < 0.05$) of control mock-transfected levels (Fig. 6*A*). As mentioned previously, the transfection efficiency in OK cells under these conditions is of the order of 30–50%; therefore, the ~35% reduction in albumin uptake observed in the total population of cells underestimates the true reduction in albumin uptake in cells overexpressing LIMK-1. This finding compares with the reduction of TR-albumin uptake to 10.0 ± 2.0% of control values ($n = 4$; $p < 0.05$) in cells pre-treated with the actin depolymerizing agent latrunculin A (Fig. 6*B*). Using the single cell confocal-based assay, we observed that fluorescein isothiocyanate-albumin uptake was effectively abolished in LLC-PK1 cells overexpressing LIMK-1 ($n = 10$, Fig. 6*B*). A time course comparing fluorescein isothiocyanate-albumin uptake in cells with different treatments to inhibit uptake is shown in (Fig. 6*B*). In addition, in the cells overexpressing LIMK-1, there was no significant change in the degree of co-localization between phosphorylated cofilin and ClC-5. The percentage of co-local-

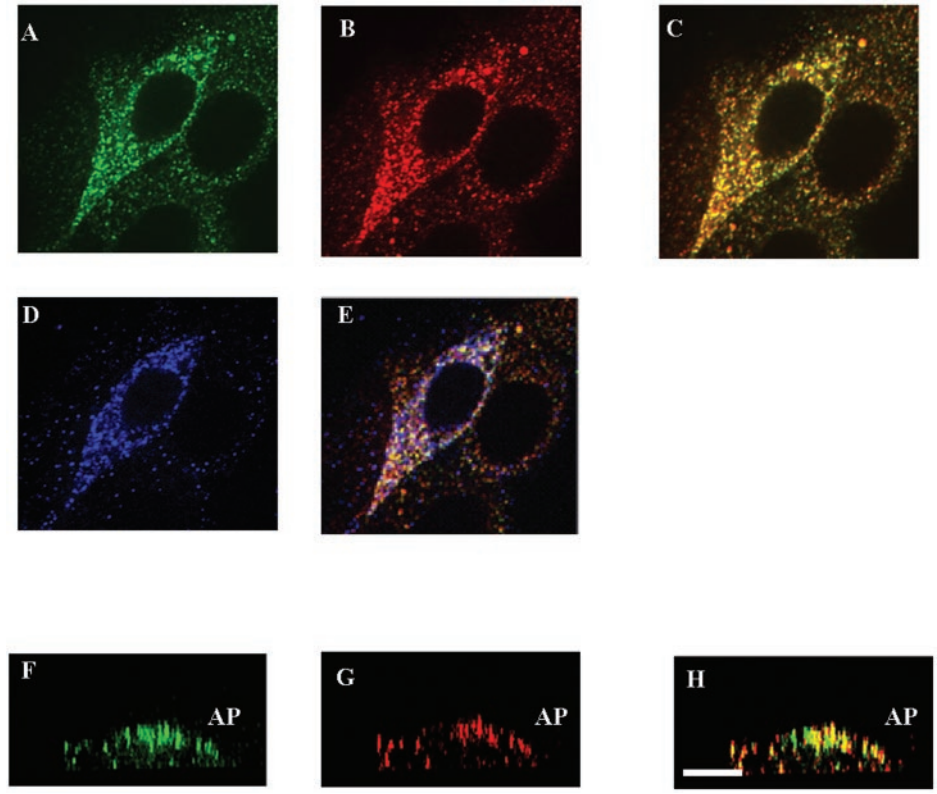

FIG. 3. **ClC-5 and cofilin co-localization in LLC-PK1 cells.** Confocal microscopy showing endogenous distribution of cofilin and ClC-5 in LLC-PK1 cells. *A*, cofilin distribution (*green*). *B*, ClC-5 distribution (*red*). *C*, merger of images in *A* and *B* clearly indicate areas of co-localization (*yellow*) between ClC-5 and cofilin. *D*, AP-2 distribution (*blue*). *E*, merger of images in *A*, *B*, and *C* showing areas of co-localization (*white*) with ClC-5 and cofilin. *F*, *z* axis scan showing the distribution of cofilin (*red*) in the apical domain. *G*, *z* axis scan showing the distribution of ClC-5 concentrated in the apical (*AP*) region. *H*, merger of images in *F* and *G* showing co-localization of cofilin and ClC-5 (*yellow*) in the apical region of the cells. *Bar*, 10 μM.

ization in LIMK-1-transfected cells was 48 ± 4% (n = 8) compared with 63.0 ± 12% (n = 8; p = NS) in control cells.

DISCUSSION

There is increasing evidence that the interactions of the C-terminal tails of ion channels and transporters with other cellular proteins are critical for many plasma membrane-associated functions. These include regulating the trafficking of the proteins to and from recycling endosomes (10, 13, 32), targeting the channels for destruction (33), forming macromolecular complexes by means of scaffold proteins that may be anchored to the cytoskeleton, or conferring spatial specificity on signal transduction from receptors (34). In this study, we used the C terminus of ClC-5 in a yeast two-hybrid screen and GST-fusion protein pulldown assay to demonstrate a physical interaction between the actin binding protein cofilin and the C-terminal tail of ClC-5. Furthermore, we showed strong co-localization of cofilin with ClC-5 in cultured cells of proximal tubule origin, indicating functional interaction in native cells. Finally, these data revealed a novel role for cofilin in the regulation of receptor-mediated albumin endocytosis in mammalian proximal tubule cells.

Interactions with the cytoskeleton are essential for the regulation of ion transport activity and trafficking, control of vesicle movement, and endocytosis, as well as assembly of signaling complexes and other macromolecular complexes at the plasma membrane (10, 13, 34). These interactions involve actin binding proteins and scaffold proteins as well as other molecules that regulate the dynamics of actin microfilament formation (for review, see Ref. 35). The apical membranes of polarized epithelial cells have complex structures composed of actin and actin binding proteins that include the core of the microvillus, the cytoskeletal terminal web underneath the plasma membrane, and the tight junctional complex that mediates cell-cell adhesion (22). There are also very high levels of endocytosis associated with the uptake of proteins from the glomerular filtrate and, therefore, in proximal tubule cells, the actin at the microvillar core and in the terminal actin web must be in a constant state of remodeling. The importance of an intact actin cytoskeleton in albumin uptake by proximal tubule cells has been demonstrated previously (3, 9).

Cofilin is a ubiquitously expressed member of the cofilin/actin-depolymerizing factor family of actin-associated proteins (36) that binds to both filamentous (F-actin) and monomeric (G-actin) actin to stimulate depolymerization of the actin microfilaments (25). Importantly, cofilin is a terminal effector of signaling cascades that evoke cytoskeletal rearrangement; cofilin has been shown to be essential for endocytosis in yeast (37). One way by which the actin filament-severing activity of cofilin is terminated is by phosphorylation at Ser^3 by LIM kinase (31, 38).

Cofilin has been reported to interact directly with one other membrane transport protein. Kim *et al.* (39) showed that the α subunit of the Na^+-K^+-ATPase binds cofilin by means of interactions with the residues Asp^{672} and Arg^{700} of the third cytoplasmic domain and, by using confocal immunofluorescence, that cofilin and Na^+-K^+-ATPase co-localized in COS-7 cells (40). In this study, we divided the C-terminal tail of ClC-5 into three separate domains of ~40–50 residues in length. These fragments contained a number of charged residues that could potentially bind cofilin; however, we were unable to detect the binding of cofilin to these constructs. This suggests that, similar to the Na^+-K^+-ATPase, the cofilin binding sites in ClC-5

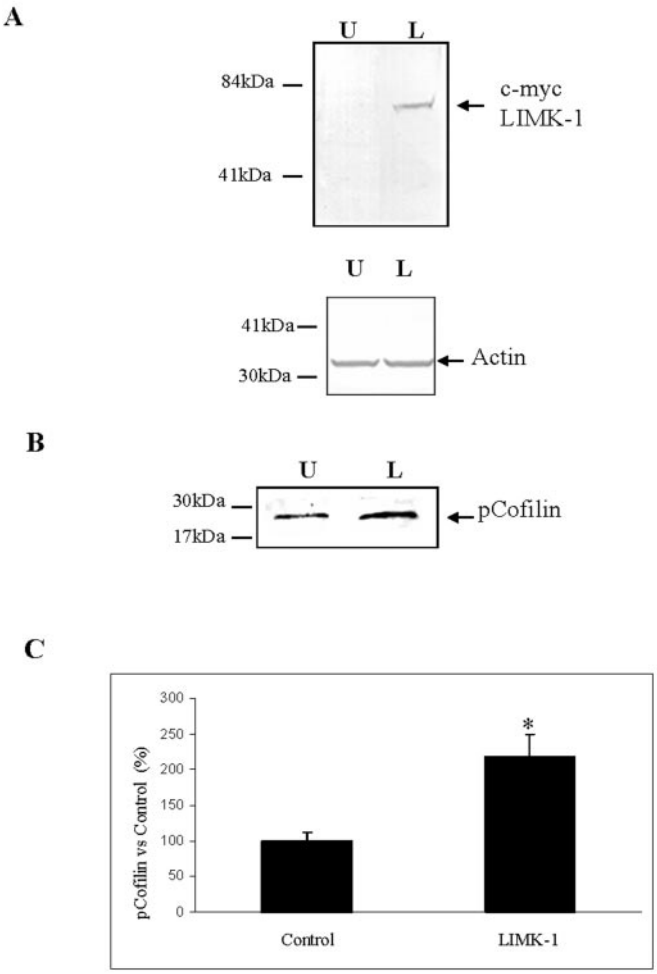

FIG. 4. **Phosphorylation of cofilin by LIMK-1 in LLC-PK1 cells.** *A*, Western blot of lysate from cells transfected with c-*myc*-tagged LIMK-1. *Upper panel*, expression of c-*myc* LIMK-1 in transfected (*L*) but not untransfected control cells (*U*). *Lower panel*, Western blot for actin shows equal loading of protein in each lane. *B*, Western blot of cell lysate showing an increase in the levels of phosphorylated cofilin (*pCofilin*) in LIMK-1-transfected cells compared with untransfected controls. *C*, densitometric analysis showing a statistically significant increase (*, $p < 0.05$; $n = 3$) in the levels of phosphorylated cofilin in cells expressing LIMK-1.

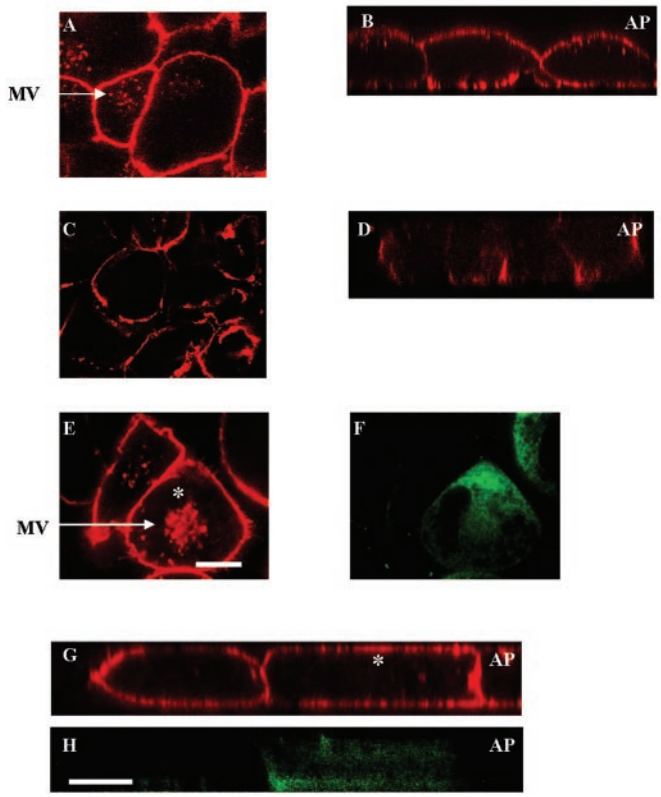

FIG. 5. **Actin distribution in OK cells transfected with LIMK-1 or treated with latrunculin A.** Actin was visualized in confluent OK cells with TRITC-phalloidin using confocal microscopy. These images are representative of three separate experiments. *A*, untransfected cells showing actin staining of both the peripheral corona and the filaments at the base of the microvilli (*MV*). *B*, *z* axis scan showing distribution of actin at both the apical and basolateral membrane domains. *C*, disruption of actin filaments after treatment with latrunculin A (10 μM) for 1 h. *D*, *z* axis scan showing loss of filamentous actin at the apical and basolateral membrane domains. *E*, actin staining in a LIMK-1 transfected cell (*) shows increased staining at the base of the microvilli (*MV*), indicating stabilization of the cytoskeleton in this region. *Bar*, 10 μM. *F*, Cy2 (*green*) staining of c-*myc* epitope in cells in *E* to identify cells expressing LIMK-1. *G*, *z* axis scan showing increased apical actin staining in a LIMK-1 transfected cell (*) compared with untransfected control. *H*, Cy2 (*green*) staining of c-*myc* epitope in cells in *G* to identify cells expressing LIMK-1. *Bar*, 10 μM.

may be relatively distant from each other in the protein.

A physiological role for the interaction of cofilin with Na^+-K^+-ATPase was demonstrated by overexpressing cofilin in COS-7 cells, which resulted in an increase in the activity of Na^+-K^+-ATPase (40). This effect was attributed to the following: (i) cofilin providing a necessary interface between the cytoskeleton and the Na^+-K^+-ATPase to allow more pump molecules to be present in the plasma membrane; or (ii) cofilin acting to localize Na^+-K^+-ATPase molecules to specific membrane regions or to anchor other regulatory proteins to enhance pump activity (40). Subsequently, Lee and co-workers (41) found that, in addition to Na^+-K^+-ATPase, cofilin also interacted with the glycolytic enzyme triose-phosphate isomerase by means of a Rho-dependent pathway. This led them to hypothesize that these interactions provided a framework to feed the Na^+-K^+-ATPase with glycolytic ATP that, in turn, enhanced the pump activity. Importantly, they also showed that cofilin did not interact with other membrane transporters such as GLUT1, GLUT4, CFTR, or plasma membrane Ca^{2+}-ATPase (41). Other evidence for the role of cofilin in regulating the behavior of ion-transporting proteins comes from a study in guinea pig cardiomyocytes, where cytochalsin D was found to reduce L-type Ca^{2+} currents (42). The investigators found that cytochalasin D treatment caused a 50% reduction in the ratio of phosphorylated to total cofilin content of the heart and concluded that cofilin regulation of F-actin polymerization state plays an important role in regulating the activity of these Ca^{2+} channels. These studies assign specific roles for cofilin in regulating ion transport at the plasma membrane. Further support for a role for actin binding proteins in mediating transport in epithelial cells comes from studies in intestinal cells, where stimulation with carbachol results in a redistribution of villin and F-actin and a reduction in apical NHE3 (43). It is also known that Rho regulates the activity of NHE3 (11), and it has been speculated that this may be by means of a cofilin-dependent mechanism (43).

The data from the current study identify a new role for cofilin in regulating albumin uptake in established cell models of the proximal tubule. Increasing the levels of phosphorylated cofilin in cells overexpressing LIM kinase and stabilizing the actin microfilaments resulted in a significant reduction in albumin uptake by both OK and LLC-PK1 cells, as measured by two different assay systems. We also demonstrate that preventing actin polymerization with latrunculin A or cytochalasin D almost totally abolished albumin uptake in these cells. These

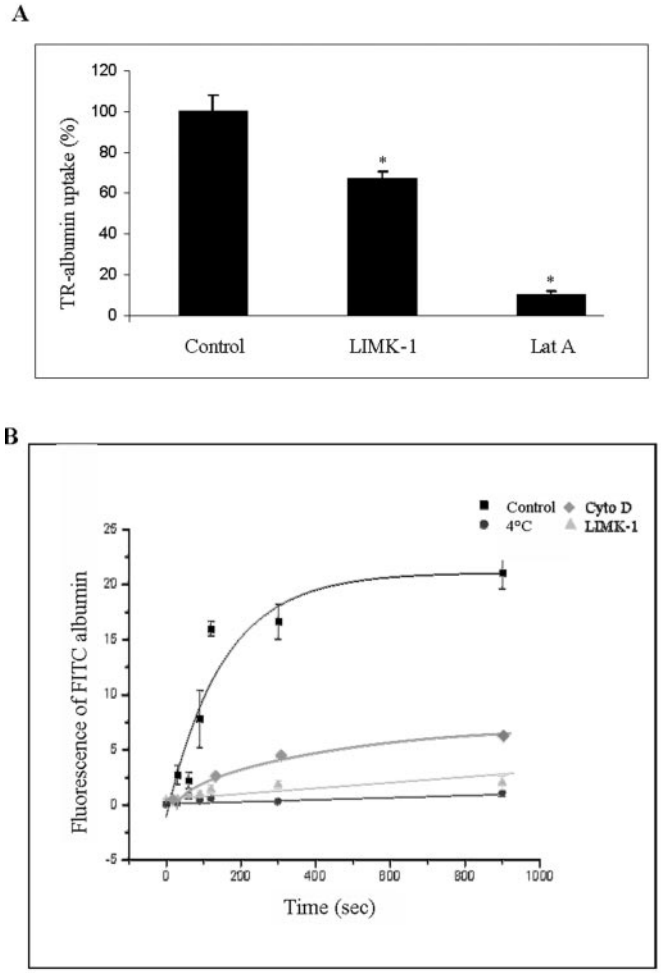

FIG. 6. **Phosphorylation of cofilin inhibits albumin endocytosis.** *A*, albumin uptake in confluent monolayers of OK cells. OK cells were transiently transfected with LIMK-1 for 7 days and exposed to TR-albumin (100 μg/ml) for 2 h. TR-albumin uptake was significantly (*, $p < 0.05$; $n = 4$) inhibited in OK cells treated with latrunculin A (1.5 μM for 30 min). *B*, albumin uptake in single LLC-PK1 cells transfected with LIMK-1. Cells were exposed to 10 mg/ml of fluorescein isothiocyanate-albumin, and uptake was detected in individual cells. Fluorescein isothiocyanate-albumin rapidly accumulated in control cells (■). Expression of LIMK-1 (▲), treatment with cytochalasin D (▲) (10 μM for 40 min), or incubation at 4 °C (●) resulted in significant decreases in albumin uptake (*, $p < 0.05$; $n = 10$).

data are consistent with the previously observed effects of cytoskeletal disruption on albumin uptake in OK cells (9). Importantly, our data demonstrate the crucial role for actin remodeling within the context of an intact cytoskeleton in endocytosis in the proximal tubule. Albumin uptake is inhibited by either stabilization of the actin microfilaments (LIMK-1 overexpression) or disruption of the actin cytoskeleton by latrunculin A or cytochalasin D.

The data presented here are the first to show that phosphorylation of cofilin by LIM kinase in two model proximal tubule cell lines significantly inhibits the uptake (endocytosis) of albumin. Although LIMK-1 was previously thought to be the "neuronal" isoform, our demonstration that OK cells express the mRNA for LIMK-1 is in agreement with a recent study that revealed the presence of both isoforms of LIM kinase in mesangial cells (44). Overexpression of LIM kinase in OK cells resulted in a stabilization of the actin cytoskeleton, as revealed by confocal microscopy, and the inhibition of albumin uptake indicates the need for extensive localized remodeling of actin to enable endocytosis to occur (22, 24). Furthermore, our data indicating that phosphorylated cofilin continues to co-localize with ClC-5 suggest that this association is maintained throughout the endocytotic cycle.

Our data provide an additional explanation for the pronounced failure of albumin endocytosis mediated by defective ClC-5 trafficking/channel function in Dent's disease and highlight the obligate role of ClC-5 in albumin endocytosis in the proximal tubule. There is some debate as to whether ClC-5 is present at the plasma membrane in epithelial cells, as the electrophysiological evidence is not solid. However, surface biotinylation experiments[2] indicate the presence of ClC-5 at the cell surface. The important point from this study is that, in terms of our model, because the C-terminal tail of ClC-5 may act to mediate the assembly and formation of the endocytic complex (thereby, correctly targeting megalin/cubulin (19) and H^+-ATPase (18)), the Cl^- transporting function of ClC-5 at the plasma membrane may be redundant. We propose that the interaction of cofilin with ClC-5 at the plasma membrane plays a crucial role in mediating actin depolymerization, thus leading to a highly localized dissolution of the terminal actin web and facilitating budding of the endosome from the plasma membrane. These findings also highlight the involvement of ClC-5 as a structural component of the endocytotic apparatus rather than its ion channel activity. Our data are consistent with the overall concept and models where localized actin depolymerization is required for endocytosis and the fact that the area in the immediate vicinity of clathrin-coated pits are devoid of actin (24).

Dent's disease mutations fall broadly into two categories. They are either non-sense mutations resulting in truncations or loss of functional protein, or they are mis-sense mutations that typically reduce the Cl^- current (*e.g.* see Ref. 45). Thus, our findings suggest that, in addition to the defect in acidification of the endosomes (as would be expected from mutations with reduced Cl^- currents) (6), the endocytotic failure arising from trafficking mutations of ClC-5 may result from the inability of the other proteins involved in albumin uptake to interact with cofilin and enable efficient movement of the nascent endosome through the cortical actin web. This model explains our previous data in ClC-5 knockout mice where the endocytosis appeared to be inhibited at the initial formation of the endosome rather than at a downstream early endosomal stage, where failure of acidification would be expected to be inhibiting endocytosis (7). It is important to note that H^+-ATPase is not required for acidification of the nascent endosome (9, 46, 47), an observation that supports a role for ClC-5 other than that as an anion shunt. The novel role we have identified for cofilin will be important in understanding the complex process of albumin uptake by the proximal tubule and the mechanisms by which it is altered in pathophysiological states.

Acknowledgments—We thank Dr. Doug Murphy for his assistance with the analysis of the endocytosis data. The c-*myc*-tagged form of LIMK-1 in pCDNA3 was generously provided by Dr. Pico Caroni (Friedrich Miescher Institute, Switzerland), and the anti-phosphorylated cofilin antibody was provided by Dr. James Bamburg (Colorado State University, Fort Collins, CO).

REFERENCES

1. Christensen, E., and Birn, H. (2001) *Am. J. Physiol.* **280,** F562–F573
2. Jentsch, T., Friedrich, T., Schriever, A., and Yamada, H. (1999) *Pfluegers Arch. Eur. J. Physiol.* **437,** 783–795
3. Gekle, M., Serrano, O. K., Drumm, K., Mildenberger, S., Freudinger, R., Gassner, B., Jansen, H. W., and Christensen E. I. (2002) *Am. J. Physiol.* **283,** F549–F558
4. Marshansky, V., Ausiello, D. A., and Brown, D. (2002) *Curr. Opin. Nephrol. Hypertens.* **11,** 527–537
5. Devuyst, O., Christie, P. T., Courtoy, P. J., Beauwens, R., and Thakker, R. V. (1999) *Hum. Mol. Genet.* **8,** 247–257

[2] D. H. Hryciw, Y. Wang, and W. B. Guggino, unpublished data.

6. Piwon, N., Gunther, W., Schwake, M., Bosl, M. R., and Jentsch, T. J. (2000) *Nature* **408,** 369–373
7. Wang, S. S., Devuyst, O., Courtoy, P. J., Wang, X. T., Wang, H., Wang, Y., Thakker, R. V., Guggino, S., and Guggino, W. B. (2000) *Hum. Mol. Genet.* **9,** 2937–2945
8. Drumm, K., Gassner, B., Silbernagl, S., and Gekle, M. (2001) *Eur. J. Med. Res.* **6,** 422–432
9. Gekle, M., Mildenberger, S., Freudinger, R., Schwerdt, G., and Silbernagl, S. (1997) *Am. J. Physiol.* **272,** F668–F677
10. Kim, J., Lee-Kwon, W., Park, J. B., Ryu, S. H., Yun, C. H., and Donowitz, M. (2002) *J. Biol. Chem.* **277,** 23714–23724
11. Kurashima, K., D'Souza, S., Szaszi, K., Ramjeesingh, R., Orlowski, J., and Grinstein, S. (1999) *J. Biol. Chem.* **274,** 29843–29849
12. Weinman, E., Steplock, D., and Shenolikar, S. (2001) *Kidney Int.* **60,** 450–454
13. Kurashima, K., Szabo, E. Z., Lukacs, G., Orlowski, J., and Grinstein, S. (1998) *J. Biol. Chem.* **273,** 20828–20836
14. Biemesderfer, D., Nagy, T., DeGray, B., and Aronson, P. S. (1999) *J. Biol. Chem.* **276,** 17518–17524
15. Bateman, A. (1997) *Trends Biochem. Sci.* **22,** 12–13
16. Ponting, C. (1997) *J. Mol. Med.* **75,** 160–163
17. Schwake, M., Friedrich, T., and Jentsch, T. J. (2001) *J. Biol. Chem.* **276,** 12049–12054
18. Moulin, P., Igarashi, T., Van Der Smissen, P., Cosyns J.-P., Verroust, P., Thakker, R., Scheinman, S. J., Courtoy, P. J., and Devuyst, O. (2003) *Kidney Int.* **63,** 1285–1295
19. Christensen, E., Devuyst, O., Dom, G., Nielsen, R., Van Der Smissen, P., Verroust, P., Leruth, M., Guggino, W. B., and Courtoy, P. J. (2003) *Proc. Natl. Acad. Sci. U. S. A.* **100,** 8472–8477
20. Zhai, X. Y., Nielsen, R., Birn, H., Drumm, K., Mildenberger, S., Freudinger, R., Moestrup, S. K., Verroust, P. J., Christensen, E. I., and Gekle, M. (2000) *Kidney Int.* **58,** 1523–1533
21. Schwegler, J., Heppelmann, B., Mildenberger, S., and Silbernagl, S. (1991) *Pfluegers Arch. Eur. J. Physiol.* **418,** 383–392
22. Apodaca, G. (2001) *Traffic* **2,** 149–159
23. Qualmann, B., Kessels, M. M., and Kelly, R. B. (2000) *J. Cell Biol.* **150,** F111–F116
24. Fujimoto, L., Roth, R., Heuser, J. E., and Schmid, S. L. (2000) *Traffic* **1,** 161–171
25. Bamburg, J. (1999) *Annu. Rev. Cell Dev. Biol.* **15,** 185–230
26. Ashworth, S. L., Southgate, E. L., Sandoval, R. M., Meberg, P. J., Bamburg, J. R., and Molitoris B. A. (2003) *Am. J. Physiol.* **284,** F852–F862
27. Wylie, F., Heimann, K., Luam Le, T., Brown, D., Rabnott, G., and Stow, J. L. (1999) *Am. J. Physiol.* **276,** C497–C506
28. Negoescu, A., Labat-Moleur, F., Lorimier, P., Lamarcq, L., Guillermet, C., Chambaz, E., and Brambilla, E. (1994) *J. Histochem. Cytochem.* **42,** 433–437
29. Meberg, P., Ono, S., Minamide, L. S., Takahashi, M., and Bamburg, J. R. (1998) *Cell Motil. Cytoskeleton* **39,** 172–190
30. Wohlfarth, V., Drumm, K., Mildenberger, S., Freudinger, R., and Gekle, M. (2003) *Kidney Int.* **84,** 103–109
31. Arber, S., Barbayannis, F. A., Hanser, H., Schneider, C., Stanyon, C. A., Bernard, O., and Caroni, P. (1998) *Nature* **393,** 805–809
32. Weinman, E. J., Minkoff, C., and Shenolikar, S. (2000) *Am. J. Physiol. Renal Physiol.* **279,** F393–F399
33. Staub, O., Gautschi, I., Ishikawa, T., Breitschopf, K., Ciechanover, A., Schild, L., and Rotin, D. (1997) *EMBO J.* **16,** 6325–6336
34. Naren, A., Cobb, B., Li, C., Roy, K., Nelson, D., Heda, G. D., Liao, J., Kirk, K. L., Sorscher, E. J., Hanrahan, J., and Clancy, J. P. (2003) *Proc. Natl. Acad. Sci. U. S. A.* **100,** 342–346
35. Brown, D., and Breton, S. (2000) *Kidney Int.* **57,** 816–824
36. Moon, A., and Drubin, D. G. (1995) *Mol. Biol. Cell* **6,** 1423–1431
37. Lappalainen, P., and Drubin, D. G. (1997) *Nature* **388,** 78–82
38. Lawler, S. (1999) *Curr. Biol.* **9,** R800–R802
39. Kim, M., Jung, J., Park, C. S., and Lee, K. (2002) *Biochimie* (*Paris*) **84,** 1021–1029
40. Lee, K., Jung, J., Kim, M., and Guidotti, G. (2001) *Biochem. J.* **353,** 377–385
41. Jung, J., Yoon, T., Choi, E. C., and Lee, K. (2002) *J. Biol. Chem.* **277,** 48931–48937
42. Rueckschloss, U., and Isenberg, G. (2001) *J. Physiol.* (*Lond.*) **537,** 363–370
43. Khurana, S. (2000) *J. Membr. Biol.* **178,** 73–87
44. Shabahang, S., Huwiler, A., and Pfeilschifter, J. (2002) *Biochem. Biophys. Res. Commun.* **298,** 408–413
45. Lloyd, S., Pearce, S. H., Fisher, S. E., Steinmeyer, K., Schwappach, B., Scheinman, S. J., Harding, B., Bolino, A., Devoto, M., Goodyer, P., Rigden, S. P., Wrong, O., Jentsch, T. J., Craig, I. W., and Thakker, R. V. (1996) *Nature* **379,** 445–449
46. Aniento, F., Gu, F., Parton, R. G., and Gruenberg, J. (1996) *J. Cell Biol.* **133,** 29–41
47. Van Deurs, B., Holm, P. K., and Sandvig, K. (1996) *Eur. J. Cell Biol.* **69,** 343–350

Cofilin Interacts with ClC-5 and Regulates Albumin Uptake in Proximal Tubule Cell Lines

Deanne H. Hryciw, Yinghong Wang, Olivier Devuyst, Carol A. Pollock, Philip Poronnik and William B. Guggino

J. Biol. Chem. 2003, 278:40169-40176.
doi: 10.1074/jbc.M307890200 originally published online August 6, 2003
